

M. MAKOWSKA-JANUSIK, I.V. KITYK, J. BERDOWSKI
and I. KASIK*

Institute of Physics WSP, PL 42 – 201, Al. Armii Krajowej 13/15, Częstochowa, Poland

PL 42 – 217 Częstochowa, Poland

** Institute of Radio Engineering and Electronics, Czech Academy of Sciences, Prague 8, Chaberska 57,
182 51, Czech Republic*

PACS 42.65 K – Second harmonic generation, optical fibres

Silica-based Materials Doped with $\text{Al}_2\text{O}_3 - \text{P}_2\text{O}_5$, Erbium and Ytterbium for Optical Fiber Drawing

Abstract: UV-photoinduced optical second harmonic generation (PISHG) in $\text{Al}_2\text{O}_3 - \text{P}_2\text{O}_5 - \text{SiO}_2$ glass doped by Er and Yb rare earths ions has been investigated. Maximal output PISHG signal is observed at time delay between the nitrogen laser ($\lambda = 337$) photoinducing and probing (YAG:Nd laser $\lambda = 1060$ nm) beams about 7 ps, at temperatures below 10K and photoinducing beam power within the $1.01 - 1.4 \text{ GW/cm}^2$. Essential influence of external electrostatic field and hydrostatic pressure on the output PISHG signal have been revealed. The Yb ions suppress the output PISHG. All the data are explained on the ground of the *ab initio* molecular dynamics simulations.

1. Introduction

Glasses of composition $\text{Al}_2\text{O}_3 - \text{P}_2\text{O}_5 - \text{SiO}_2$ doped with rare -earth are promising materials for using different optoelectronic devices [1 – 3]. Presence of the rare earth ions makes these compositions very sensitive to external UV-light illumination, because the frequencies hit directly to resonance levels 4f – 5d terms of the particular rare ions. Moreover there appears a possibility to operate by their optical parameters by the external UV-light, temperature and hydrostatic pressure fields due to the possibility a variation of the rare-earth valence states (photoinduced heterovalency) under influence of the external fields.

From general physical-chemical similarity one can expect an appearance of the UV photoinduced non-linear optics phenomena in such materials. As a consequence main goal of the present work consists in a study of the photoinduced second harmonic generation (PISHG) in these optical fibres under different external conditions (pressure, temperature).

To observe the optical second harmonic generations in the disordered (or centrosymmetric) materials usually apply photoinduced nonlinear optical methods described in the details elsewhere (see for example [4 – 6]) because the non-centrosymmetry is

a necessary condition for observation of the optical second harmonic generation described by third rank polar tensor. As a consequence the similar method will be applied for investigations of the rare-doped glasses in order to check influence of different rare earth ions on the output PISHG.

2. Experimental

As a source of the photoinduced changes UV nitrogen laser beam ($\lambda = 337$ nm) with a photon flux of $10^{17} - 10^{18}$ photons/cm² have been used. Upper power restriction was caused by a necessity to avoid sample heating. An intensity at specimen position was checked using a commercial fast-response joulemeter (Genetic, Inc., model ED – 200). More details concerning the measurement technique are given in the reference 7 and 8.

Apparatus for the SHG was supplied with an unforced beam from a single-mode picosecond YAG – Nd laser ($\lambda = 1.06$ μ m), with a power near 30 MW, pulse time duration varying within the 10 – 30 ps. The measurements were performed both for polarised as well unpolarised light beams. Separation between the output SHG and pump light was achieved using grating monochromator (spectral resolution up to 7 nm/mm). Laser beam diameter have been varied within the 20 – 1250 μ m. Such wide range of the beam diameter variation have been caused by necessity to achieve the optimal phase matching synchronism conditions for the investigated glasses.

PISHG intensity was detected using a PMD – 33M photomultiplier working in the digital quantum regime. The output signal was observed only for the effective χ_{zzz} tensor. Z-direction corresponds to polarisation of the photoinducing UV nitrogen beam. All the measurements have been started for the undoped glasses and only afterwards have been done for similar conditions for the Yb, Er-doped glasses. As a consequence comparing of the PISHG effects properly due to the rare earth presence within the similar conditions was possible. To ensure same conditions of measurements surface states, scattering losses and averaged non-homogeneity have been monitored. Moreover to eliminate non-homogeneity connected with the non-uniform distribution of the rare-earth ions averaging procedure consisting in the scanning measurements in more than 85 points of the investigated glasses have been applied. All the obtained data have been treated using the $\chi^{(2)}$ Student statistics not worse than 0.02 [8]. The measurements were done in the single-pulse regime, with a pulse frequency repetition of 12 Hz. As an intensity standard a quartz single-crystal cell in the plane of the optic axis have been used. Simultaneously for every measured point the incident angle have been varied in order to achieve the maximal phase synchronism conditions due to photoinduced changes of the refractive index. The self-focused beam diameter about 1.24 μ m was of a gaussian-like form with the half-width about 72%. Single-mode regime of laser generation have been applied to eliminate intermode competition and different kinds of soliton effects. Simultaneously the reflected optical beam (both incident as well doubled) have been controlled to extract an influence of the near-the surface effect. Time-dependent SHG signal were measured by means of the high-time-resolved spectroanalyzer SA – 107. Time synchronisation between the photoinducing and probing beams was ensured within the 200 fs.

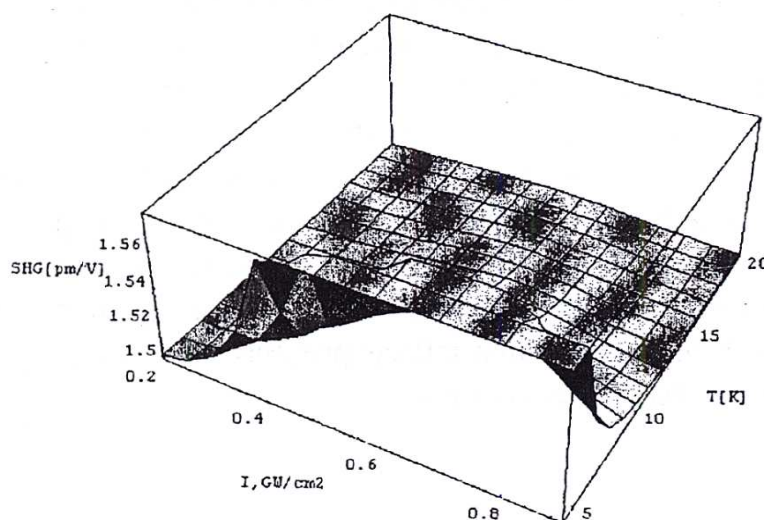
The investigating materials were of cylindrical prepared by MCVD method [9] extended by the solution-doping technique [10,11]. Composition of the samples were determined by Electron Microprobe Analysis (JEOL JxA50A) and it is presented in Table 1.

Table 1. Composition of samples

	Pure	Er doped	Er + Yb doped
Al_2O_3 [mol%]	11.3	3.1	14.7
P_2O_5 [mol%]	12.9	0	11.8
SiO_2 [mol%]	75.8	96.8	70.6
Yb^{3+} [ppm]	0	0	2500
Er^{3+} [ppm]	0	800	26 800

3. Results and discussions

From the Fig. 1 one can see that the maximal output PISHG is achieved at time shift between the pumping and probing beam about 7 ps and temperature about 4.2 K. All the data are presented after averaging over the UV-laser photoinducing beam power within the $0.8 - 1.2 \text{ GW/cm}^2$. With the next increase of the delaying time the output PISHG signal continuously decreases at least at 20%. Decreasing of the PISHG with temperature enhancement is usually explained [7,8] within a framework of the low-temperature ordering. Increasing temperature favours higher reorientation disorder that destroy all the non-centrosymmetry dipoles. At temperatures higher than 46 K the observed PISHG is equal to the scattered background. Optimal time of the pumping-probing delay indicates on essential role of the electronic subsystem in the observed effects.

**Fig. 1.** Dependence of the PISHG versus the temperature T and photoinducing flux beam at delaying time about 7 ps.

Lets consider influence of external fields, particularly of the electrostatic field with strength up to 300 kV/m (see Fig. 2). All the presented measurements are done at liquid helium temperature and are performed for the optimal delaying time between the photoinducing and probing beams (about 7 ps). From the Fig. 2 one can clearly see that the PISHG appears at the photon flux of 1.92 GW/cm^2 and electrostatic field of 200 kV/m. And at the absence of the field the PISHG is shifted up to 1.21 GW/cm^2 . Applied external electrostatic field shifts the maximum of the PISHG towards the less photoinducing beam powers. Therefore one can see that the PISHG maximum is achieved due to ordering under influence of the external electrostatic and photoinduced

beams. Each of the mentioned factors due to the different electron-phonon anharmonic interactions shows different contribution to the output PISHG. In all the cases the pure and Yb doped glasses do not show any effect. The polarisation-dependent measurements have shown that the local symmetry of the crystallites has point group C_2 .

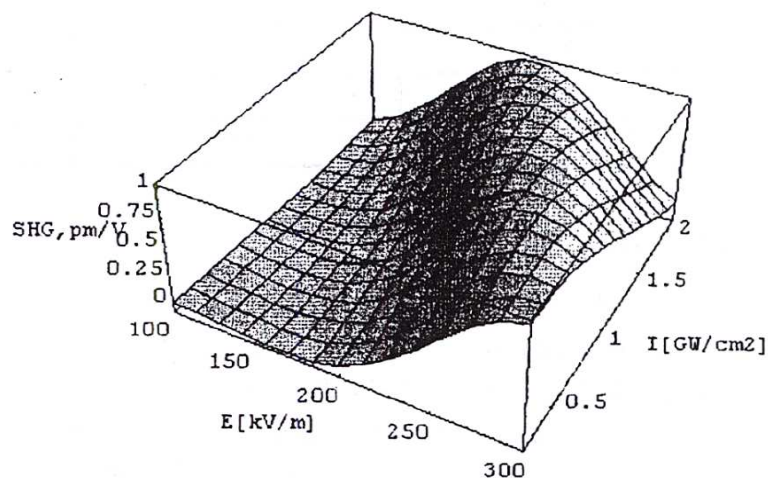


Fig. 2. Dependence of the PISHG versus the electrostatic field E and photoinducing beam intensity I at (liquid helium temperature) LHeT for the optimal photoinduced conditions.

The another important aspect consists in a possibility of varying the local non-centrosymmetry using external hydrostatic field that possess scalar symmetry. In the Fig. 3 are presented dependencies of the PISHG intensities for the $(Er^{3+} - Al_2O_3 - P_2O_5 - SiO_2)$ as a function of hydrostatic pressure at liquid nitrogen temperature. One can clearly see that maximum value of the PISHG is obtained for the pumping photon flux of 0.94 GW/cm^2 and the hydrostatic pressure of 15 GPa. The upper pressure limit is defined by mechanical stability of the specimen. With decreasing temperature or increasing pressure the PISHG increases. The resulting PISHG intensity can be explained by pressure-induced local structural non-centrosymmetry and the pressure-dependent maximum is caused by the chemical rearrangement of the $(Er^{3+} - Al_2O_3 - P_2O_5 - SiO_2)$. The remaining two specimens do not show essential PISHG signal that reflects probably the key role by the high localised $4f-5d$ Er orbitals in the observed phenomena.

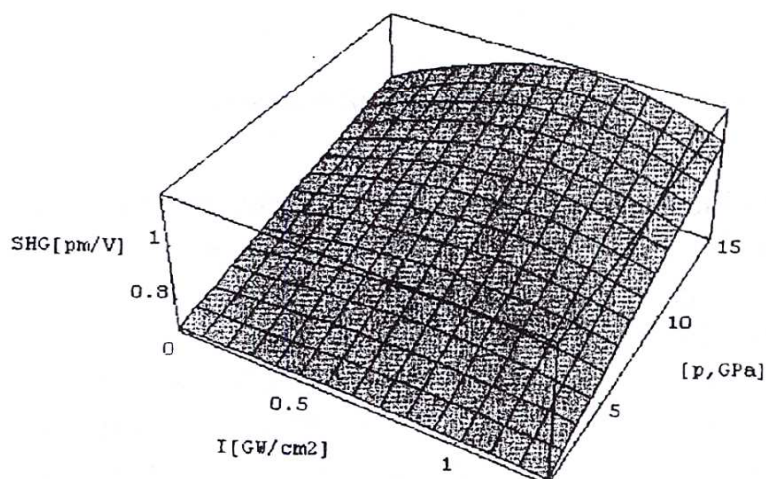


Fig. 3. Dependence of the PISHG versus photoinducing beam I and hydrostatic pressure p at (liquid nitrogen temperature) LNT.

In the Fig. 4 are presented the changes of electrostatic potential distribution within the $[SiO_4]$ clusters of the mentioned glasses under the different external conditions. Before UV-illumination we have practically symmetric $Si-O_4$ tetrahedra. In the case of the Er-doped glasses due to the mentioned photopolarisation of the Er we observe effective changes of electrostatic potential distributions with appearance of additional non-centrosymmetry (see Fig. 4b). When the Yb ions are inserted we have once more returning to the more spherical case (see for example Fig. 4c). By the arrows are shown effective phonon modes effectively contributing to the output nonlinear optical susceptibilities. Therefore addition of Yb have an effect similar as compensation of the local non-centrosymmetry typical for the pure glasses.

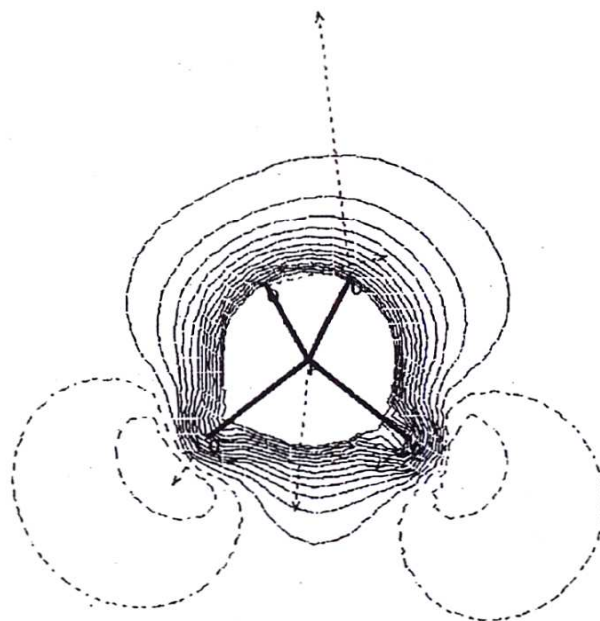


Fig. 4a. Electrostatic potential distribution within the SiO_4 tetrahedra for the different glasses under the low-temperature photoinducing illuminations — pure (undoped by the rare earth).

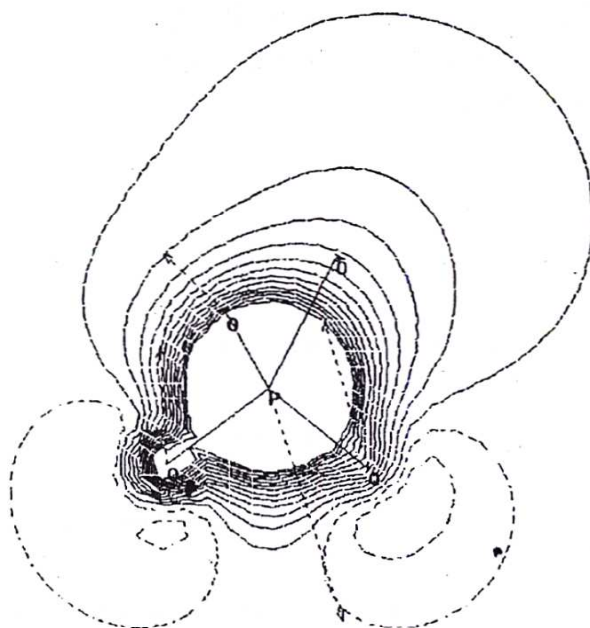


Fig. 4b. Electrostatic potential distribution within the SiO_4 tetrahedra for the different glasses under the low-temperature photoinducing illuminations — Er-doped glasses.

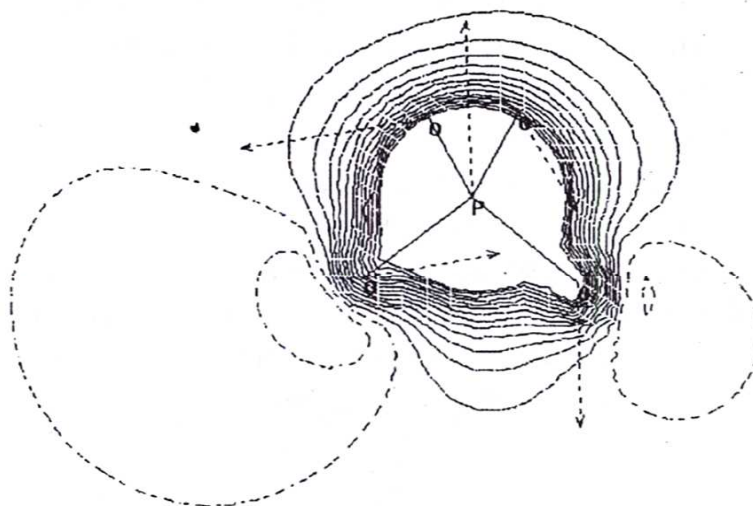


Fig. 4c. Electrostatic potential distribution within the SiO_4 tetrahedra for the different glasses under the low-temperature photoinducing illuminations — doped simultaneously by Er and Yb.

Conclusion

Studied material of rare-earth doped silica ($\text{Er}^{3+} - \text{Al}_2\text{O}_3 - \text{P}_2\text{O}_5 - \text{SiO}_2$) have been exhibited PISHG at low temperatures, high pressures or external electrostatic field. Only the erbium doped material ($\text{Er}^{3+} - \text{Al}_2\text{O}_3 - \text{P}_2\text{O}_5 - \text{SiO}_2$) exhibited PISHG on photoinducing flux and time delay (between the pumping and probing). So the erbium doped $\text{Al}_2\text{O}_3 - \text{P}_2\text{O}_5 - \text{SiO}_2$ glasses can be considered as suitable for fast-time non-linear optics. The applying external electric field shifts maximum of the PISHG towards less photoinducing beam powers achieving the maximum (about 1 pm/V) for the UV-photoinducing flux of 1.92 GW/cm^2 and the electrostatic field of 2000 kV/m. The applied hydrostatic pressure favours appearance of the maximum PISHG (1.3 pm/V) at hydrostatic pressure about 15 GPa and photoinducing beam power about 0.82 GW/cm^2 . The observed experimental dependences are explained on the ground of the *ab initio* molecular dynamics simulations.

References

- [1] M.C. Farries, M.E. Fermann, R.I. Laming, S.B. Poole and D.N. Payne, *Electron. Lett.* **22**, 418 (1986).
- [2] J. Castillo, V.P. Kozich and A. Marcano, *Optics Letters* **19**, 171 (1994).
- [3] A. Darickova, V. Matejec, M. Pospisilova, M. Chomat and I. Kasik: *proc. Photonics'95*, Prague, April 1995, p. 261.
- [4] I.V. Kityk, J. Ulanski, J.K. Jeszka and A. Tracz, *Advanced Materials for Optics and Electronics* **6**, 358 (1996).
- [5] E. Golis, I.V. Kityk, J. Wasylak and J. Kasperczyk, *Materials Research Bulletin* **31**, 1057 (1996).
- [6] R.I. Mervinskii, I.V. Kityk, M. Makowska-Janusik and J. Straube, *Non-linear Optics* **13**, 245 (1995).
- [7] J. Wasylak, J. Kucharski, I.V. Kityk and B. Sahraoui, *Journ. of Applied Physics* **85**, 425 (1999).

-
- [8] B. Sahraoui, I.V. Kityk, X. Nguyen Phu, P. Hudhomme and A. Gorgues, *Physical Review* **B59B**, 9229 (1999).
- [9] S.R. Nagel, J.B. MacChesney and K.L. Walker: *IEEE J. Quantum El.* **QE-18**, 459 (1982).
- [10] J.E. Townsend, S.B. Pool and D.N. Payne, *Electron. Lett.* **23**, 329 (1987).
- [11] V. Matejec, I. Kasik and M. Pospisilova: *J. Non-Cryst. Solids* **192&193**, 195 (1995) 195.